



Published in final edited form as:

Hepatology. 2020 August ; 72(2): 412–429. doi:10.1002/hep.31031.

Interleukin-22 ameliorates neutrophil-driven nonalcoholic steatohepatitis through multiple targets

Seonghwan Hwang¹, Yong He¹, Xiaogang Xiang¹, Wonhyo Seo¹, Seung-Jin Kim¹, Jing Ma¹, Tianyi Ren¹, Seol Hee Park¹, Zhou Zhou¹, Dechun Feng¹, George Kunos², Bin Gao^{1,*}

¹Laboratory of Liver Diseases, National Institute on Alcohol Abuse and Alcoholism, National Institutes of Health, Bethesda, MD, 20892, USA

²Laboratory of Physiologic Studies, National Institute on Alcohol Abuse and Alcoholism, National Institutes of Health, Bethesda, MD, 20892, USA

Abstract

Nonalcoholic fatty liver disease encompasses a spectrum of diseases ranging from simple steatosis to nonalcoholic steatohepatitis (NASH), cirrhosis, and liver cancer. At present, how simple steatosis progresses to NASH remains obscure and effective pharmacological therapies are lacking. Hepatic expression of C-X-C motif chemokine ligand 1 (CXCL1), a key chemokine for neutrophil infiltration (a hallmark of NASH), is highly elevated in NASH patients but not in fatty livers in obese individuals or in high-fat diet (HFD)-fed mice. Here we demonstrate that overexpression of *Cxcl1* in the liver alone promotes steatosis-to-NASH progression in HFD-fed mice by inducing neutrophil infiltration, oxidative stress, and stress kinase (such as ASK1 and p38MAPK) activation. Myeloid cell-specific deletion of the neutrophil cytosolic factor 1 (*Ncf1*)/*p47^{phox}* gene, which encodes a component of the NADPH oxidase 2 complex that mediates neutrophil oxidative burst, markedly reduced CXCL1-induced NASH and stress kinase activation in HFD-fed mice. Treatment with interleukin (IL)-22, a cytokine with multiple targets, ameliorated CXCL1/HFD-induced NASH or methionine-choline deficient diet-induced NASH in mice. Mechanistically, IL-22 blocked hepatic oxidative stress and its associated stress kinases via the induction of metallothionein, one of the most potent antioxidant proteins. Moreover, although it does not target immune cells, IL-22 treatment attenuated the inflammatory functions of hepatocyte-derived, mitochondrial DNA-enriched extracellular vesicles, thereby suppressing liver inflammation in NASH.

Conclusion: Hepatic overexpression of CXCL1 is sufficient to drive steatosis-to-NASH progression in HFD-fed mice through neutrophil-derived reactive oxygen species and activation of stress kinases, which can be reversed by IL-22 treatment via the induction of metallothionein.

Keywords

Inflammation; extracellular vesicles; oxidative stress; mitochondrial DNA

*Corresponding author: Bin Gao, M.D., Ph.D., Laboratory of Liver Diseases, NIAAA/NIH, 5625 Fishers Lane, Bethesda, MD 20892; Tel: 301-443-3998. bgao@mail.nih.gov.

Author contributions:

SH designed and conducted the experiments and wrote the paper; YH, XX, WS, SK, JM, TR, SHP, ZZ, DF conducted some experiments; GK helped experiment design, performed data analysis and edited the manuscript; BG supervised the whole project and wrote the paper.

Introduction

Nonalcoholic fatty liver disease (NAFLD) is a leading cause of chronic liver disease and ranges from simple steatosis to nonalcoholic steatohepatitis (NASH), cirrhosis, and hepatocellular carcinoma.^(1, 2) While simple steatosis is mostly devoid of inflammation and is considered benign, 10-20% of patients with fatty livers progress to NASH, which is characterized by the presence of inflammation, ballooning, hepatocyte injury, and fibrosis.^(3, 4) Despite considerable progress in our understanding of the pathogenesis of NASH, the critical factors that drive the progression of simple steatosis to NASH still remain largely unknown, and existing animal models fail to reflect the full spectrum of NAFLD progression.⁽⁵⁻⁷⁾ For example, although chronic feeding of a high-fat diet (HFD) leads to obesity and insulin resistance in mice, two crucial risk factors for NASH,⁽⁸⁾ it only mimics the gene expression profile and histopathology of simple steatosis but not those of NASH.^(5, 6)

A key feature of human NASH is a robust infiltration of neutrophils in the liver, which is not significantly observed in fatty livers in obese individuals or in HFD-fed mice.^(9, 10) The enhanced infiltration of neutrophils is in accordance with the observation that C-X-C motif chemokine ligand 1 (CXCL1), a major chemokine for neutrophil chemotaxis,⁽¹¹⁾ is one of the most highly upregulated chemokines in the liver of NASH patients but only slightly elevated in fatty livers in obese individuals and in HFD-fed mice.^(9, 10) However, it is not clear whether upregulation of hepatic CXCL1 is the major factor that drives steatosis-to-NASH progression. To answer this question, we overexpressed *Cxcl1* in the liver of HFD-fed mice and found that overexpression of *Cxcl1* was sufficient to induce NASH phenotypes in HFD-fed mice, as evidenced by significant elevation of serum alanine aminotransferase (ALT), liver inflammation, and fibrosis. In addition, *Cxcl1*-overexpressing livers displayed elevated levels of reactive oxygen species (ROS) and activation of several stress kinases, including apoptosis signal-regulating kinase 1 (ASK1), p38 mitogen-activated protein kinase (MAPK), and c-Jun N-terminal kinase (JNK). It is believed that aberrant infiltration of neutrophils exacerbates hepatocyte injury, liver inflammation, and fibrosis in the course of NAFLD through the production of ROS, release of proteases, neutrophil extracellular traps (NETs), and secretion of inflammatory factors.^(3, 12) However, the exact role of neutrophils in promoting steatosis-to-NASH progression remains unknown. In the current paper, by using several strains of knockout mice, we demonstrate that neutrophil cytosolic factor 1 (*Ncf1*), which encodes p47^{phox}, an important component of NADPH oxidase 2 complex that mediates neutrophil oxidative burst,⁽¹³⁾ contributes to CXCL1-induced liver injury and fibrosis in HFD-fed mice.

NASH is a complex disease and multiple therapeutic targets have been proposed and are currently being evaluated in clinical trials, including steatosis, oxidative stress, hepatocyte death, inflammation, and fibrosis.^(1, 14) Due to many drivers of NASH pathogenesis, combination therapies or a single drug with multiple targets will likely achieve greater therapeutic efficacy than engaging a single target.^(1, 14) Interestingly, interleukin (IL)-22 seems to be an ideal drug with multiple beneficial effects including anti-steatotic, anti-apoptotic, anti-oxidative, anti-fibrotic, and pro-regenerative functions in the liver.⁽¹⁵⁾ These

beneficial effects are mainly due to IL-22 activation of the signal transducer and activator of transcription 3 (STAT3) pathway in hepatocytes.⁽¹⁵⁾ More importantly, IL-22 specifically targets epithelial cells including hepatocytes without affecting immune cells due to expression of its receptor IL-22R1 restricted to epithelial cells.^(15, 16) Phase I clinical trials revealed that IL-22 had minimal side effects in healthy individuals.⁽¹⁷⁾ IL-22 improved fatty liver in HFD-fed mice,⁽¹⁸⁾ but its effect on NASH has not been tested. In the current study, we have set out to test whether IL-22Fc treatment can ameliorate CXCL1-induced NASH in HFD-fed mice. IL-22Fc is a recombinant fusion protein that consists of two IL-22 molecules bound to an immunoglobulin constant region (IgG2-Fc), resulting in an extended half-life.⁽¹⁷⁾ Our data revealed that IL-22Fc treatment ameliorated CXCL1-induced NASH in HFD-fed mice or NASH in methionine-choline deficient diet (MCD)-fed mice, suggesting the therapeutic potential of IL-22Fc for the treatment of NASH. Mechanistically, IL-22Fc treatment highly upregulated hepatic antioxidant enzymes, metallothionein (MT) 1 and MT2, two proteins that scavenge hydroxyl and superoxide radicals and are 800 times more potent than glutathione in preventing hydroxyl radical-induced DNA damage.⁽¹⁹⁾ By inducing hepatic MTs, IL-22Fc was able to attenuate hepatic ROS production, stress kinase activation, and the inflammatory functions of hepatocyte-derived extracellular vesicles (EVs), thereby ameliorating CXCL1-driven NASH.

Materials and Methods

Mice

C57BL/6J, *Mt1/2^{-/-}*, *Elane^{-/-}*, *Pad4* floxed, and Lysozyme M Cre mice were obtained from the Jackson Laboratory (Bar Harbor, ME). *Ask1^{-/-}* mice were originally obtained from Dr. Hidenori Ichijo (University of Tokyo, Japan)⁽²⁰⁾ and kindly provided by Dr. Peixin Yang (University of Maryland, Baltimore, MD). For *Ask1^{-/-}* and *Elane^{-/-}* mice, heterozygous mice were bred to generate knockout mice and their corresponding WT littermate controls. *Mt1/2^{-/-}* mice with deletion of both *Mt1* and *Mt2* genes were backcrossed to a C57BL/6N background for more than 15 generations, and C57BL/6N mice were used as controls. *Ncf1* floxed mice were generated by Applied StemCell (Milpitas, CA). *Ncf1* floxed mice and *Pad4* floxed mice were crossed with Lysozyme M Cre mice via several steps to delete *Ncf1* or *Pad4* in myeloid-derived cells, respectively.

Generation of CXCL1-induced NASH in HFD-fed mice

Male mice (6–7 weeks of age) were fed an HFD (60 kcal% fat; D12492, Research Diets, New Brunswick, NJ) or a chow diet (10 kcal% fat) for 3 months and injected via tail vein with Ad-*Gfp* or Ad-*Cxcl1* (Applied Biological Materials, Richmond, Canada). Mice were continued on the HFD or chow diet for 2, 4, or 8 weeks after the adenovirus infection, then were sacrificed for analysis. To test the efficacy of IL-22Fc (kindly provided by Generon Corporation, Shanghai, China) or GS-4997 (Selleckchem, Houston, TX), mice were injected intraperitoneally with IL-22Fc (0.5 mg/kg) on days 3 and 10 post adenoviral infection, while GS-4997 (4 mg/kg) was injected intraperitoneally on days 7, 9, 11, and 13 post adenoviral infection. Isotype IgG2 control for IL-22Fc was obtained from BioLegend (San Diego, CA). All mice were maintained in accordance with NIH guidelines. The study was approved by the NIAAA Animal Care and Use Committee.

Statistical analysis

Data are expressed as mean \pm SEM and were analyzed using GraphPad Prism software (v. 7.0a; GraphPad Software, La Jolla, CA). To compare values obtained from two groups, the Student's t-test was performed. Data from multiple groups were compared with one-way ANOVA followed by Tukey's post hoc test. *P* values of <0.05 were considered significant.

Results

Overexpression of *Cxcl1* alone promotes steatosis-to-NASH progression in HFD-fed mice

CXCL1 is highly upregulated in human NASH,⁽⁹⁾ which was confirmed by immunohistochemistry analyses in Fig. 1A, but not in human fatty liver⁽⁹⁾ or HFD-induced fatty liver in mice.⁽²¹⁾ To determine whether overexpression of CXCL1 alone can induce NASH phenotype in HFD-fed mice, C57BL/6 mice were fed an HFD for 3 months followed by a 2-week infection with an adenoviral vector that overexpresses CXCL1 (Ad-*Cxcl1*) or a control vector encoding GFP protein (Ad-*Gfp*). We confirmed the upregulation of CXCL1 in the liver sections and the serum of mice and elevation of hepatic neutrophil infiltration post Ad-*Cxcl1* infection (Supporting Fig. S1A–D). Neither body weight nor liver weight was affected by Ad-*Cxcl1* infection (Supporting Fig. S1A). Hepatic overexpression of CXCL1 alone in HFD-fed mice recapitulated the pathological features of human NASH such as steatosis, liver injury, inflammation, and fibrosis, as demonstrated by serum ALT measurement, RT-qPCR analyses, and immunohistochemistry, which was not observed in Ad-*Gfp*-infected, HFD-fed mice (Fig. 1B–C, Supporting Fig. S1E). Hepatic overexpression of CXCL1 in chow-fed mice did not generate NASH phenotype because of the lack of steatosis and fibrosis despite serum ALT elevation, albeit to a lesser extent compared with that in HFD-fed mice, and hepatic infiltration of neutrophils and macrophages (Supporting Fig. S2A–B). Finally, the NASH-inducing effect of Ad-*Cxcl1* was sustained 2, 4, and 8 weeks post infection in HFD-fed mice, as evidenced by significant fibrosis, inflammation, and liver injury (Fig. 1D, Supporting Fig. S3A–F).

Analysis of the published human microarray data⁽²²⁾ revealed 1022 genes whose expression was increased by greater than 1.5-fold in the livers of NASH patients (n=16) compared with those of simple steatosis (n=10). These genes were subjected to Gene Enrichment and Functional Annotation analysis using DAVID Gene Functional Classification Tool (<https://david.ncifcrf.gov>), which demonstrated a notable enrichment of genes involved in inflammation and fibrosis (Supporting Fig. S4A). We further tested whether the livers of CXCL1-overexpressing mice possess a similarity in inflammatory and fibrotic gene expression pattern to the livers of NASH patients. To this end, we selected 48 human genes that were included in more than one category of the enriched functions and/or have well-established association with inflammation and fibrosis to perform RT-qPCR analysis of their mouse homologs. Remarkably, all these 48 inflammatory and fibrogenic genes were upregulated in the liver of Ad-*Cxcl1*-infected, HFD-fed mice (Fig. 1E, Supporting Fig. S4B), suggesting that hepatic overexpression of CXCL1 alone mimicked hepatic gene expression profiles of NASH patients and thus may serve as a useful tool for studying the molecular pathogenesis of NASH as well as identifying a novel therapeutic target.

Neutrophil infiltration mediates CXCL1-induced liver injury in HFD-fed mice via p47^{phox}-dependent mechanisms

Although neutrophil infiltration is a hallmark of NASH, the role of neutrophils in the pathogenesis of NASH still remains obscure. Here we used this CXCL1-induced NASH model to study the role of neutrophils in inducing liver injury and fibrosis in NASH. As activated neutrophils produce ROS through oxidative burst, we performed immunohistochemical analysis of malondialdehyde (MDA) and 4-hydroxynonenal (4-HNE) and revealed that CXCL1 overexpression elevated oxidative stress in both chow- and HFD-fed mice (Fig. 2A, Supporting Fig. S5A). Hepatic overexpression of CXCL1 in HFD-fed mice increased the mRNA levels of NADPH oxidase 2 (gp91^{phox}) and NADPH oxidase 2 complex components, which mediate neutrophil oxidative burst (Fig. 2B).⁽²³⁾

ASK1 is an MAPK kinase kinase that mediates ROS-induced cell death through activation of stress kinases such as p38 and JNK.⁽²⁴⁾ We tested whether CXCL1-induced oxidative stress leads to activation of ASK1, p38, or JNK. Hepatic expressions of p-ASK1 and p-p38 were significantly increased (Fig. 2C). We then examined whether neutrophil oxidative burst is responsible for CXCL1-induced activation of ASK1 and p38 by a transwell migration assay in which AML12 mouse hepatocytes were cocultured with bone marrow-derived neutrophils (Fig. 2D). CXCL1 significantly increased the chemotaxis of neutrophils toward the bottom chamber and the phosphorylation of ASK1 and p38 in AML12 cells, which was repressed by diphenyleneiodonium (DPI), an inhibitor of NADPH oxidase (Fig. 2D, Supporting Fig. S5B).

To verify that neutrophil-derived oxidative stress contributes to the liver damage in the CXCL1-overexpressing liver, we generated myeloid cell-specific *Ncf1* knockout (*Ncf1*^{Ly2z-/-}) mice. Lysozyme M Cre-mediated deletion of the *Ncf1* gene in myeloid cells led to a reduction in expression of NCF1 in bone marrow-derived neutrophils (Fig. 2E, Supporting Fig. S5C). HFD-fed *Ncf1*^{Ly2z-/-} mice showed a reduction in serum ALT levels, a fibrosis marker alpha smooth muscle actin (α -SMA), and phosphorylation of ASK1 and p38 compared with HFD-fed wild-type (WT) mice at 2 weeks after Ad-*Cxcl1* infection (Fig. 2E–F, Supporting Fig. S5D–E). However, the mRNA levels of collagen genes and Sirius Red staining were comparable between these two groups (Supporting Fig. S5D–E). These findings indicate that neutrophil-derived NCF1/p47^{phox}-dependent ROS plays an important role in CXCL1-induced NASH by activating ASK1, p38, and JNK. In contrast, deletion of the *Ncf1* gene in myeloid cells did not affect serum ALT levels in MCD-fed mice (Supporting Fig. S5F), indicating that neutrophil-derived ROS does not contribute to liver injury in this model, which may be attributed to the significant difference between MCD model and human NASH with the latter being associated with significant hepatic neutrophil infiltration that promotes liver injury.⁽⁶⁾

We also tested whether CXCL1 overexpression exacerbates liver injury through other mechanisms that contribute to neutrophil activation such as elastase activity and NET formation.⁽²⁵⁾ ALT levels were not affected by deletion of the *Elane* gene (encoding elastase) or inhibition of NET formation through myeloid cell-specific deletion of the *Pad4* gene (encoding peptidylarginine deiminase 4) or treatment of NET inhibitor Cl-amidine

(Supporting Fig. S6A–C), indicating that elastase or NET formation does not contribute to CXCL1-induced NASH.

IL-22Fc therapy ameliorates liver injury, inflammation, and fibrosis in CXCL1/HFD-induced NASH and MCD-induced NASH in mice

Using the CXCL1/HFD-induced NASH model, we sought to identify a drug candidate that can ameliorate NASH caused by neutrophil-derived oxidative stress. IL-22 is a hepatoprotective cytokine that is known to upregulate potent antioxidant enzymes, MT1 and MT2.⁽²⁶⁾ Also, IL-22 has been shown to improve HFD-induced obesity, insulin resistance, and hepatic fat accumulation;⁽¹⁸⁾ however, the HFD-induced obesity model rarely causes NASH in mice and thus it is unknown whether IL-22 can also protect against NASH-associated liver inflammation and fibrosis. Therefore, here we tested whether IL-22Fc possesses a therapeutic potential to improve neutrophil-driven NASH in mice (Supporting Fig. S7A). IL-22Fc therapy reduced serum ALT levels to the extent that was comparable to the value of Ad-*Gfp*-infected mice (Fig. 3A). Reduced hepatocyte death was further confirmed by terminal deoxynucleotidyl transferase dUTP nick end labeling (TUNEL) (Supporting Fig. S8A). Also, IL-22Fc decreased oxidative stress and apoptosis in the liver as evidenced by a reduction in MDA- and 4-HNE-positive area (Fig. 3B, Supporting Fig. S8A), phosphorylation of stress kinases (ASK1 and p38), and caspase-3 (CASP3) cleavage (Fig. 3C). Consequently, IL-22Fc reduced hepatic F4/80-positive area and the formation of hepatic crown-like structures (Fig. 3D–E), which are indicative of macrophage aggregates surrounding the lipid-laden hepatocytes and crucially involved in NASH-associated inflammation.⁽²⁷⁾ IL-22Fc also reduced hepatic fibrogenesis as illustrated by a reduction in Sirius Red- and α -SMA-positive area (Fig. 3D–E). Reduction in inflammation and fibrosis was further confirmed by RT-qPCR analysis of inflammatory and fibrogenic genes (Fig. 3F). IL-22Fc reduced liver weight but not body weight (Supporting Fig. S7B). IL-22Fc did not reduce the hepatic expression of CXCL1, serum levels of CXCL1, or CXCL1-induced neutrophil infiltration (Supporting Fig. S8A–D).

Furthermore, IL-22Fc reduced liver injury and fibrosis in mice with NASH induced by 6-week MCD feeding (Supporting Fig. S9A–C), suggesting that IL-22Fc has a therapeutic potential in other NASH models with different pathogenic mechanisms.

IL-22 protection against NASH is independent of ASK1, a stress kinase that is only partially involved in CXCL1-induced liver injury but not fibrosis

Activation of ASK1 has been implicated in the pathogenesis of early NAFLD in experimental models,^(24, 28) and the above data show that IL-22Fc attenuated ASK1 activation in neutrophil-driven NASH. We wondered whether ASK1 activation is involved in the development of neutrophil-driven NASH, and IL-22Fc ameliorates it via an ASK1-dependent mechanism. Pharmacological inhibition of ASK1 by GS-4997 partially repressed CXCL1-induced elevation of serum ALT levels (Fig. 4A) and suppressed ASK1-activated stress kinases, CASP3 cleavage, and oxidative stress (Supporting Fig. S10A–B), but inflammation and fibrosis were not attenuated by GS-4997 (Fig. 4B, Supporting Fig. S11A–B). Similar results were also obtained from the studies of *Ask1*^{-/-} mice (Fig. 4A, Fig. 4C, Supporting Fig. S12A). Altogether, our data suggest that ASK1 inhibition only moderately

mitigates the liver injury with minimal beneficial effects on liver inflammation and fibrosis in this neutrophil-driven NASH model, which may explain the failure of the recent clinical trial using anti-ASK1 therapy for the treatment of patients with severe NASH.

Furthermore, IL-22Fc treatment in *Ask1*^{-/-} mice reduced serum ALT levels as it does in WT mice (Fig. 4D), indicating that ASK1 inhibition is not required for the ability of IL-22Fc to attenuate liver injury. Consistently, IL-22Fc treatment caused similar inhibition of H₂O₂-induced death and CASP3 cleavage of *Ask1*^{-/-} and WT hepatocytes (Supporting Fig. S13A–B). Collectively, these data indicate that IL-22Fc attenuates ROS-induced liver injury at the hepatocyte level independently of ASK1 modulation.

IL-22 protects against NASH progression in an MT-dependent manner

To better understand how IL-22Fc attenuates CXCL1-induced NASH phenotypes, we sought to identify the mechanism by which IL-22Fc represses oxidative stress in the liver. In line with our previous microarray analysis which demonstrated that the antioxidant genes *Mt1* and *Mt2* are the two most highly upregulated genes in the liver from IL-22 transgenic mice, (26) IL-22Fc remarkably elevated the mRNA levels of *Mt1* and *Mt2* in the liver (Fig. 5A) and their protein expression (Fig. 5B). To determine whether IL-22Fc lowers ROS levels in hepatocytes, we performed a flow cytometric analysis of dichlorofluorescein (DCF) fluorescence. H₂O₂ increased the intensity of DCF fluorescence, which was inhibited by IL-22Fc in both AML12 cells (Fig. 5C) and mouse primary hepatocytes (Fig. 5D). Intriguingly, IL-22Fc failed to reduce ROS levels in *Mt1/2*^{-/-} hepatocytes, suggesting that IL-22Fc lowers ROS levels through the action of MTs (Fig. 5D). Moreover, IL-22Fc inhibited H₂O₂-induced phosphorylation of ASK1 and p38, CASP3 cleavage, and cell death in WT but not in *Mt1/2*^{-/-} hepatocytes (Fig. 5E–F, Supporting Fig. S14A–B). Pharmacological inhibition of p38 by LY2228820 or PH797804 prevented H₂O₂- or TNF- α -induced hepatocyte death (Supporting Fig. S14C), indicating that p38 inhibition by IL-22Fc contributes to its hepatocyte-protective effect. These collectively indicate that IL-22Fc ameliorates oxidative stress and hepatocyte death through the upregulation of MTs and the subsequent inhibition of ASK1, p38, and CASP3 cleavage.

The critical role of MTs in IL-22Fc protection against ROS-induced hepatocyte death prompted us to determine whether IL-22Fc attenuates NASH phenotypes through MT upregulation *in vivo* as well. First, IL-22Fc reduced ALT levels in WT mice but not in *Mt1/2*^{-/-} mice (Fig. 6A, Supporting Fig. S15A). Also, IL-22Fc failed to reduce oxidative stress in *Mt1/2*^{-/-} mice, as evidenced by the staining of MDA and 4-HNE (Fig. 6B, Supporting Fig. S15C). The ability of IL-22Fc to inhibit the phosphorylation of ASK1 and p38 and the cleavage of CASP3 was blunted in the liver of *Mt1/2*^{-/-} mice (Fig. 6C). Moreover, the expression of inflammatory genes was decreased upon IL-22Fc administration, which was not observed in *Mt1/2*^{-/-} mice (Fig. 6D). Deletion of the *Mt1* and *Mt2* genes also impaired the ability of IL-22Fc to suppress the expression of fibrogenic genes (Fig. 6E). However, deletion of *Mt1* and *Mt2* did not affect the ability of IL-22Fc to reduce liver weight, suggesting that anti-steatotic effect of IL-22Fc is not mediated by MTs (Supporting Fig. S15B). Taken together, MT induction is the key mechanism underlying the anti-NASH effect of IL-22Fc.

IL-22 suppresses hepatic inflammation by modulating inflammatory property of EVs released from damaged hepatocytes in an MT-dependent manner

While IL-22R1 is expressed in hepatocytes but not in immune cells, we explored the possibility that IL-22Fc ameliorates NASH not only through the direct inhibition of hepatocyte injury but also by modulating inflammation, presumably through the crosstalk between hepatocytes and immune cells. EV has been recently highlighted as an intercellular messenger that can alter the function of recipient cells. In particular, damaged hepatocytes release inflammatory EVs and promote NASH progression via the activation of macrophages.^(29, 30) Indeed, treatment with EVs from H₂O₂-treated hepatocytes markedly upregulated the expression of inflammatory genes in RAW264.7 cells compared to treatment with EVs from vehicle-treated hepatocytes; however, EVs from IL-22Fc-pretreated hepatocytes caused less induction of these genes (Fig. 7A). The identity of EVs was confirmed by immunoblot analyses of EV marker proteins such as CD63 and ALIX, and their sizes ranged from 50 nm to 200 nm (Supporting Fig. S16). Intriguingly, EVs from *Mt1/2*^{-/-} hepatocytes pretreated with IL-22Fc retained the ability to induce inflammatory genes in RAW264.7 cells, suggesting a critical role of MTs in modulating inflammatory properties of EVs (Fig. 7A).

The above data suggest that IL-22Fc treatment inhibits the pro-inflammatory functions of EVs from H₂O₂-treated hepatocytes. Next, we asked whether IL-22Fc inhibition of inflammatory EVs was due to inhibition of EV release from hepatocytes or alteration of the inflammatory content in EVs. As illustrated in Fig. 7B, IL-22Fc treatment did not affect H₂O₂-stimulated EV release from mouse primary hepatocytes. We then postulated that IL-22Fc may alter the functional properties of EV contents rather than the degree of EV release. As damaged cells release greater amount of oxidized mitochondrial DNA (mtDNA) via EVs which in turn activates immune cells,⁽³¹⁾ we performed qPCR analysis of genes existing in the mitochondrial genome (e.g., *Atp6*, *Cox3*, and *Nd2*) using DNA isolated from EVs as a means to measure the amount of mtDNA in EVs.^(32, 33) H₂O₂ treatment elevated the levels of mitochondrial genes in EVs released from WT hepatocytes, which were reduced by IL-22Fc; however, the ability of IL-22Fc to decrease the mtDNA inclusion in EVs was blunted in *Mt1/2*^{-/-} hepatocytes (Fig. 7C). As it is known that mtDNA stimulates inflammation via Toll-like receptor 9 (TLR9) in the development of NASH,⁽³⁰⁾ we tested whether EVs released from H₂O₂-damaged hepatocytes activate RAW264.7 cells through TLR9. Treatment of RAW264.7 cells with a TLR9 antagonist ODN2088 attenuated the upregulation of inflammatory genes by EVs released from H₂O₂-treated hepatocytes (Fig. 7D).

In vivo, CXCL1 overexpression in HFD-fed mice markedly increased the mtDNA inclusion in the serum EVs, which was reversed by IL-22Fc treatment (Fig. 7E). IL-22Fc reduction of mtDNA content in the EVs was blunted in *Mt1/2*^{-/-} mice (Fig. 7F). Overall, these data indicate that oxidative stress causes hepatocytes to release mtDNA-enriched inflammatory EVs, and IL-22Fc represses the inflammatory functions of EVs in an MT-dependent manner.

Discussion

There are two key findings in the current study. First, hepatic overexpression of *Cxcl1* is sufficient to promote the progression of steatosis to NASH. Second, IL-22, a single drug with multiple targets, ameliorated CXCL1/HFD-induced NASH and MCD-induced NASH in mice.

Overexpression of CXCL1 alone induces neutrophil-driven NASH in HFD-fed mice: a critical role of neutrophil-derived, p47^{phox}-dependent ROS production

Neutrophil infiltration is a hallmark of NASH but the roles of neutrophils in NASH development remain obscure. Here we provided several lines of evidence suggesting that neutrophils promote NASH development via the production of ROS that activates several stress kinases in the liver. First, hepatic overexpression of CXCL1 in HFD-fed mice dramatically expanded the hepatic neutrophil population, exacerbated oxidative stress, and activated ROS-sensitive kinase ASK1, which in turn activated downstream p38/JNK-CASP3 pathway and resulted in liver injury, inflammation, and fibrosis (Fig. 8). Second, at the hepatocyte level, CXCL1-induced neutrophil infiltration increased phosphorylation of ASK1, p38, and JNK, which was attenuated by pharmacological inhibition of NADPH oxidase involved in neutrophilic ROS production. Third, *Ncf1^{Lyz-/-}* mice exhibited a reduction in CXCL1-induced phosphorylation of ASK1, p38, and JNK, liver injury, and fibrosis compared with WT mice. Because *Ncf1/p47^{phox}* is predominantly expressed in neutrophils and plays a key role in generating oxidative burst by neutrophils,⁽²³⁾ the observed phenotypes in *Ncf1^{Lyz-/-}* mice were likely mainly due to deletion of *Ncf1* in neutrophils. This altogether indicates that ROS production by infiltrating neutrophils is the crucial initiator for the series of detrimental events observed in CXCL1-induced NASH. While CXCL1 primarily stimulates the recruitment of neutrophils by binding to CXCR2, it should be noted that CXCR2-expressing monocytes can be also recruited by CXCL1 and thus may also contribute, at least in part, to CXCL1-induced NASH development.

One limitation of the current model is that adenoviral overexpression of CXCL1 leads to high levels of CXCL1 which are far greater than those observed in NASH patients. However, as there are a large number of chemokines for neutrophil chemotaxis besides CXCL1 (e.g., CXCL6, IL-8, CCL2, CCL3, CCL5, etc) that are elevated in NASH patients, it is very likely that overexpression of a single chemokine, CXCL1, up to high levels is necessary for achieving sufficient neutrophil infiltration when other neutrophil chemokines are not elevated. Using this model meets the goal of this study which is to test the concept that neutrophil infiltration (a hallmark of human NASH) is crucial for the progression of fatty liver to NASH.

IL-22Fc, a single drug with multiple targets, ameliorates neutrophil-driven NASH: involvement of induction of MTs that reduce ROS

The pathogenesis of NASH involves multiple drivers such as steatosis, oxidative stress, hepatocyte apoptosis, inflammation, and fibrosis.⁽¹⁾ Hence, a therapeutic option that targets multiple aspects in the pathogenesis of NASH is considered to have the potential to be

efficacious; however, therapeutic candidates with multiple targets have been rarely investigated for the treatment of NASH.

Previous studies have documented the metabolic benefits of IL-22 in obese mice (e.g., improvement of fatty liver, hyperglycemia, and insulin resistance).^(18, 34) However, these studies were not suitable to explore the anti-inflammatory or anti-fibrotic effects of IL-22 in the liver, due to the weak induction of inflammation and fibrosis in simple obesity. The present study revealed additional benefits of IL-22 in CXCL1-induced NASH besides its anti-steatotic function such as mitigating liver injury, oxidative stress, hepatic inflammation and fibrosis, demonstrating that IL-22Fc therapy can target the majority of the pathogenic mechanisms and thus can be a potent and promising option for the treatment of NASH. Furthermore, our data suggest that these beneficial effects of IL-22Fc are achieved through a mechanism involving the two potent antioxidant enzymes, MT1 and MT2. Previous studies on the hepatoprotective effect of IL-22 mostly addressed the contribution of regenerative and proliferative genes, while little focus has been given to the anti-oxidative capacity of IL-22, although MT1 and MT2 are highly upregulated in IL-22 transgenic mice.⁽²⁶⁾ The current study provides several lines of evidence suggesting that induction of MT1 and MT2 is the key mechanism underlying the anti-NASH effect of IL-22. First, IL-22Fc upregulated MT1 and MT2 and decreased oxidative stress in the liver caused by CXCL1 overexpression. Second, in H₂O₂-treated hepatocytes, IL-22Fc reduced ROS levels, phosphorylation of ROS-activated kinases such as ASK1 and p38, and apoptotic signaling in an MT-dependent manner. Lastly, deletion of *Mt1* and *Mt2* impaired the ability of IL-22Fc to attenuate inflammation and fibrosis in mouse liver.

IL-22Fc suppresses inflammation by modulating the pro-inflammatory functions of hepatocyte-derived EVs via the induction of MTs

While IL-22 is known to protect against tissue damage, it also possesses pro-inflammatory properties by stimulating epithelial cells to produce inflammatory mediators under certain conditions.⁽¹⁵⁾ However, in the current study, our data revealed that IL-22Fc treatment clearly reduced liver inflammation in CXCL1-induced NASH. As IL-22 does not act on immune cells, it is reasonable to speculate that the anti-inflammatory effect of IL-22Fc stems from the removal of the inflammatory cue originating from non-immune cells such as damaged hepatocytes. Indeed, our data revealed that IL-22Fc treatment attenuated the inclusion of proinflammatory mtDNA in hepatocyte EVs released upon oxidative stress both *in vitro* and *in vivo*. The ability of IL-22Fc to reduce the inflammatory property of EVs was dependent on MTs, in accordance with the finding that IL-22Fc suppresses ROS-induced hepatocyte damage in an MT-dependent manner. Collectively, our data suggest a novel role of IL-22Fc in modulation of inflammation.

ASK1 is dispensable for the anti-NASH effect of IL-22Fc

While ASK1 has recently drawn attention as a potential therapeutic target for NASH treatment, recent phase III clinical trials of the most advanced ASK1 inhibitor, selonsertib (GS-4997), failed due to the insufficient improvement in fibrosis. In our study using CXCL1-induced NASH, we observed virtually no improvement in inflammation or fibrosis by selonsertib administration, which is reminiscent of its failure in the clinical trials

although the early events happening in NASH pathogenesis such as hepatocellular injury and oxidative stress were mildly improved by ASK1 inhibition. This indicates that ASK1 inhibition could presumably attenuate the early drivers of NASH but not reverse the inflammation/fibrosis established in NASH.

The anti-NASH effects of IL-22Fc are independent of ASK1 although IL-22Fc treatment inhibits ASK1 in the liver. It is logical to assume that CXCL1-induced NASH can activate not only ASK1 but also other ROS-activated kinases (e.g., MEKKs and MLKs) that relay signal to apoptosis activation via p38 and JNK.⁽³⁵⁾ In contrast to ASK1-inhibiting therapy, IL-22Fc ameliorated NASH by reducing ROS levels which could subsequently repress not only ASK1 but also other ROS-activated kinases that accelerate NASH progression.

Therapeutic potential of IL-22Fc for the treatment of NASH

Although serum IL-22 levels are increased in patients with liver cirrhosis of diverse etiology,⁽³⁶⁾ it is predicted that IL-22Fc therapy can be an effective option for NASH based on multiple evidence. First, IL-22Fc administration to healthy individuals increased the serum IL-22 levels to as high as 200,000 pg/mL, which is ~1,000 times greater than its level observed in cirrhotic patients (~200 pg/mL) and implies that the pharmacological benefit of IL-22Fc can trump pathological function of elevated levels of endogenous IL-22.⁽³⁶⁾ Second, a phase I clinical trial revealed that IL-22Fc is safe and well-tolerated with favorable pharmacodynamic properties such as an induction of acute phase proteins.⁽¹⁷⁾ Lastly, a phase IIb trial demonstrated the safety and efficacy of IL-22Fc in patients with severe alcoholic hepatitis.⁽³⁷⁾ The limited side effect of IL-22Fc treatment observed in healthy volunteers and patients was probably due to the restricted expression of IL-22 receptor in epithelial cells but not in immune cells.

In conclusion, it is highly anticipated that IL-22 therapy can effectively mitigate NASH with limited side effects, considering the recent clinical trials and our pharmacological and mechanistic data obtained in mice.

Supplementary Material

Refer to Web version on PubMed Central for supplementary material.

Acknowledgement

We greatly appreciate Generon Corporation (Shanghai, China) for providing IL-22Fc recombinant protein, Dr. Hidenori Ichijo (University of Tokyo, Japan) for giving us permission to use *Ask1*^{-/-} mice, and Dr. Peixin Yang (University of Maryland, Baltimore, MD) for providing the mice.

Financial support:

This work was supported by the intramural program of NIAAA, NIH (B.G.)

Abbreviations:

ALT	alanine aminotransferase
ASK1	apoptosis signal-regulating kinase 1

CASP3	caspase-3
CXCL1	C-X-C motif chemokine ligand 1
DCF	dichlorofluorescein
DPI	diphenyleneiodonium
EV	extracellular vesicle
HFD	high-fat diet
4-HNE	4-hydroxynonenal
IL	interleukin
JNK	c-Jun N-terminal kinase
MAPK	mitogen-activated protein kinase
MCD	methionine choline-deficient diet
MDA	malondialdehyde
MPO	myeloperoxidase
MT	metallothionein
mtDNA	mitochondrial DNA
NAFLD	nonalcoholic fatty liver disease
NASH	nonalcoholic steatohepatitis
NCF1	neutrophil cytosolic factor 1
NET	neutrophil extracellular trap
ROS	reactive oxygen species
STAT3	signal transducer and activator of transcription 3
TLR9	Toll-like receptor 9
TUNEL	terminal deoxynucleotidyl transferase dUTP nick end labeling
WT	wild-type

References

Author names in bold designate shared co-first authorship.

- 1). Friedman SL, Neuschwander-Tetri BA, Rinella M, Sanyal AJ. Mechanisms of NAFLD development and therapeutic strategies. *Nat Med* 2018;24:908–922. [PubMed: 29967350]
- 2). Ibrahim SH, Hirsova P, Gores GJ. Non-alcoholic steatohepatitis pathogenesis: sublethal hepatocyte injury as a driver of liver inflammation. *Gut* 2018;67:963–972. [PubMed: 29367207]

- 3). Gao B, Tsukamoto H. Inflammation in Alcoholic and Nonalcoholic Fatty Liver Disease: Friend or Foe? *Gastroenterology* 2016;150:1704–1709. [PubMed: 26826669]
- 4). Tilg H, Moschen AR. Evolution of inflammation in nonalcoholic fatty liver disease: the multiple parallel hits hypothesis. *Hepatology* 2010;52:1836–1846. [PubMed: 21038418]
- 5). Farrell G, Schattenberg JM, Leclercq I, Yeh MM, Goldin R, Teoh N, et al. Mouse Models of Nonalcoholic Steatohepatitis: Toward Optimization of Their Relevance to Human Nonalcoholic Steatohepatitis. *Hepatology* 2019;69:2241–2257. [PubMed: 30372785]
- 6). Teufel A, Itzel T, Erhart W, Brosch M, Wang XY, Kim YO, et al. Comparison of Gene Expression Patterns Between Mouse Models of Nonalcoholic Fatty Liver Disease and Liver Tissues From Patients. *Gastroenterology* 2016;151:513–525.e510. [PubMed: 27318147]
- 7). Brenner DA. Of Mice and Men and Nonalcoholic Steatohepatitis. *Hepatology* 2018;68:2059–2061. [PubMed: 30033687]
- 8). Sanyal AJ. Past, present and future perspectives in nonalcoholic fatty liver disease. *Nat Rev Gastroenterol Hepatol* 2019;16:377–386. [PubMed: 31024089]
- 9). Bertola A, Bonnafous S, Anty R, Patouraux S, Saint-Paul MC, Iannelli A, et al. Hepatic expression patterns of inflammatory and immune response genes associated with obesity and NASH in morbidly obese patients. *PLoS One* 2010;5:e13577. [PubMed: 21042596]
- 10). Chang B, Xu MJ, Zhou Z, Cai Y, Li M, Wang W, et al. Short- or long-term high-fat diet feeding plus acute ethanol binge synergistically induce acute liver injury in mice: an important role for CXCL1. *Hepatology* 2015;62:1070–1085. [PubMed: 26033752]
- 11). Kolaczowska E, Kubes P. Neutrophil recruitment and function in health and inflammation. *Nat Rev Immunol* 2013;13:159–175. [PubMed: 23435331]
- 12). van der Windt DJ, Sud V, Zhang H, Varley PR, Goswami J, Yazdani HO, et al. Neutrophil extracellular traps promote inflammation and development of hepatocellular carcinoma in nonalcoholic steatohepatitis. *Hepatology* 2018;68:1347–1360. [PubMed: 29631332]
- 13). Bedard K, Krause KH. The NOX family of ROS-generating NADPH oxidases: physiology and pathophysiology. *Physiol Rev* 2007;87:245–313. [PubMed: 17237347]
- 14). Rotman Y, Sanyal AJ. Current and upcoming pharmacotherapy for non-alcoholic fatty liver disease. *Gut* 2017;66:180–190. [PubMed: 27646933]
- 15). Sabat R, Ouyang W, Wolk K. Therapeutic opportunities of the IL-22-IL-22R1 system. *Nat Rev Drug Discov* 2014;13:21–38. [PubMed: 24378801]
- 16). Gao B, Xiang X. Interleukin-22 from bench to bedside: a promising drug for epithelial repair. *Cell Mol Immunol* 2019;16:666–667. [PubMed: 29921965]
- 17). Tang KY, Lickliter J, Huang ZH, Xian ZS, Chen HY, Huang C, et al. Safety, pharmacokinetics, and biomarkers of F-652, a recombinant human interleukin-22 dimer, in healthy subjects. *Cell Mol Immunol* 2019;16:473–482. [PubMed: 29670279]
- 18). Yang L, Zhang Y, Wang L, Fan F, Zhu L, Li Z, et al. Amelioration of high fat diet induced liver lipogenesis and hepatic steatosis by interleukin-22. *J Hepatol* 2010;53:339–347. [PubMed: 20452699]
- 19). Abel J, de Ruiter N. Inhibition of hydroxyl-radical-generated DNA degradation by metallothionein. *Toxicol Lett* 1989;47:191–196. [PubMed: 2545017]
- 20). Tobiume K, Matsuzawa A, Takahashi T, Nishitoh H, Morita K, Takeda K, et al. ASK1 is required for sustained activations of JNK/p38 MAP kinases and apoptosis. *EMBO Rep* 2001;2:222–228. [PubMed: 11266364]
- 21). Wang W, Xu MJ, Cai Y, Zhou Z, Cao H, Mukhopadhyay P, et al. Inflammation is independent of steatosis in a murine model of steatohepatitis. *Hepatology* 2017;66:108–123. [PubMed: 28220523]
- 22). Lake AD, Novak P, Fisher CD, Jackson JP, Hardwick RN, Billheimer DD, et al. Analysis of global and absorption, distribution, metabolism, and elimination gene expression in the progressive stages of human nonalcoholic fatty liver disease. *Drug Metab Dispos* 2011;39:1954–1960. [PubMed: 21737566]
- 23). El-Benna J, Dang PM, Gougerot-Pocidalo MA, Marie JC, Braut-Boucher F. p47phox, the phagocyte NADPH oxidase/NOX2 organizer: structure, phosphorylation and implication in diseases. *Exp Mol Med* 2009;41:217–225. [PubMed: 19372727]

- 24). Schuster S, Feldstein AE. NASH: Novel therapeutic strategies targeting ASK1 in NASH. *Nat Rev Gastroenterol Hepatol* 2017;14:329–330. [PubMed: 28377639]
- 25). Honda M, Kubes P. Neutrophils and neutrophil extracellular traps in the liver and gastrointestinal system. *Nat Rev Gastroenterol Hepatol* 2018;15:206–221. [PubMed: 29382950]
- 26). Park O, Wang H, Weng H, Feigenbaum L, Li H, Yin S, et al. In vivo consequences of liver-specific interleukin-22 expression in mice: Implications for human liver disease progression. *Hepatology* 2011;54:252–261. [PubMed: 21465510]
- 27). Itoh M, Kato H, Suganami T, Konuma K, Marumoto Y, Terai S, et al. Hepatic crown-like structure: a unique histological feature in non-alcoholic steatohepatitis in mice and humans. *PLoS One* 2013;8:e82163. [PubMed: 24349208]
- 28). Zhang P, Wang PX, Zhao LP, Zhang X, Ji YX, Zhang XJ, et al. The deubiquitinating enzyme TNFAIP3 mediates inactivation of hepatic ASK1 and ameliorates nonalcoholic steatohepatitis. *Nat Med* 2018;24:84–94. [PubMed: 29227477]
- 29). Hirsova P, Ibrahim SH, Krishnan A, Verma VK, Bronk SF, Werneburg NW, et al. Lipid-Induced Signaling Causes Release of Inflammatory Extracellular Vesicles From Hepatocytes. *Gastroenterology* 2016;150:956–967. [PubMed: 26764184]
- 30). Garcia-Martinez I, Santoro N, Chen Y, Hoque R, Ouyang X, Caprio S, et al. Hepatocyte mitochondrial DNA drives nonalcoholic steatohepatitis by activation of TLR9. *J Clin Invest* 2016;126:859–864. [PubMed: 26808498]
- 31). Nakayama H, Otsu K. Mitochondrial DNA as an inflammatory mediator in cardiovascular diseases. *Biochem J* 2018;475:839–852. [PubMed: 29511093]
- 32). Cai Y, Xu MJ, Koritzinsky EH, Zhou Z, Wang W, Cao H, et al. Mitochondrial DNA-enriched microparticles promote acute-on-chronic alcoholic neutrophilia and hepatotoxicity. *JCI Insight* 2017;2:e92634.
- 33). Seo W, Gao Y, He Y, Sun J, Xu H, Feng D, et al. ALDH2 deficiency promotes alcohol-associated liver cancer by activating oncogenic pathways via oxidized DNA enriched extracellular vesicles. *J Hepatol* 2019;71:1000–1011. [PubMed: 31279903]
- 34). Wang X, Ota N, Manzanillo P, Kates L, Zavala-Solorio J, Eidenschenk C, et al. Interleukin-22 alleviates metabolic disorders and restores mucosal immunity in diabetes. *Nature* 2014;514:237–241. [PubMed: 25119041]
- 35). Son Y, Kim S, Chung HT, Pae HO. Reactive oxygen species in the activation of MAP kinases. *Methods Enzymol* 2013;528:27–48. [PubMed: 23849857]
- 36). Kronenberger B, Rudloff I, Bachmann M, Brunner F, Kapper L, Filmann N, et al. Interleukin-22 predicts severity and death in advanced liver cirrhosis: a prospective cohort study. *BMC Med* 2012;10:102. [PubMed: 22967278]
- 37). Arab JP, Sehwat T, Simonetto DA, Verma V, Feng D, Tang T, et al. An Open Label, Cohort Dose Escalation Study to Assess the Safety and Efficacy of IL-22 Agonist F-652 in Patients with Alcoholic Hepatitis. *Hepatology* 2018;68:1454A.

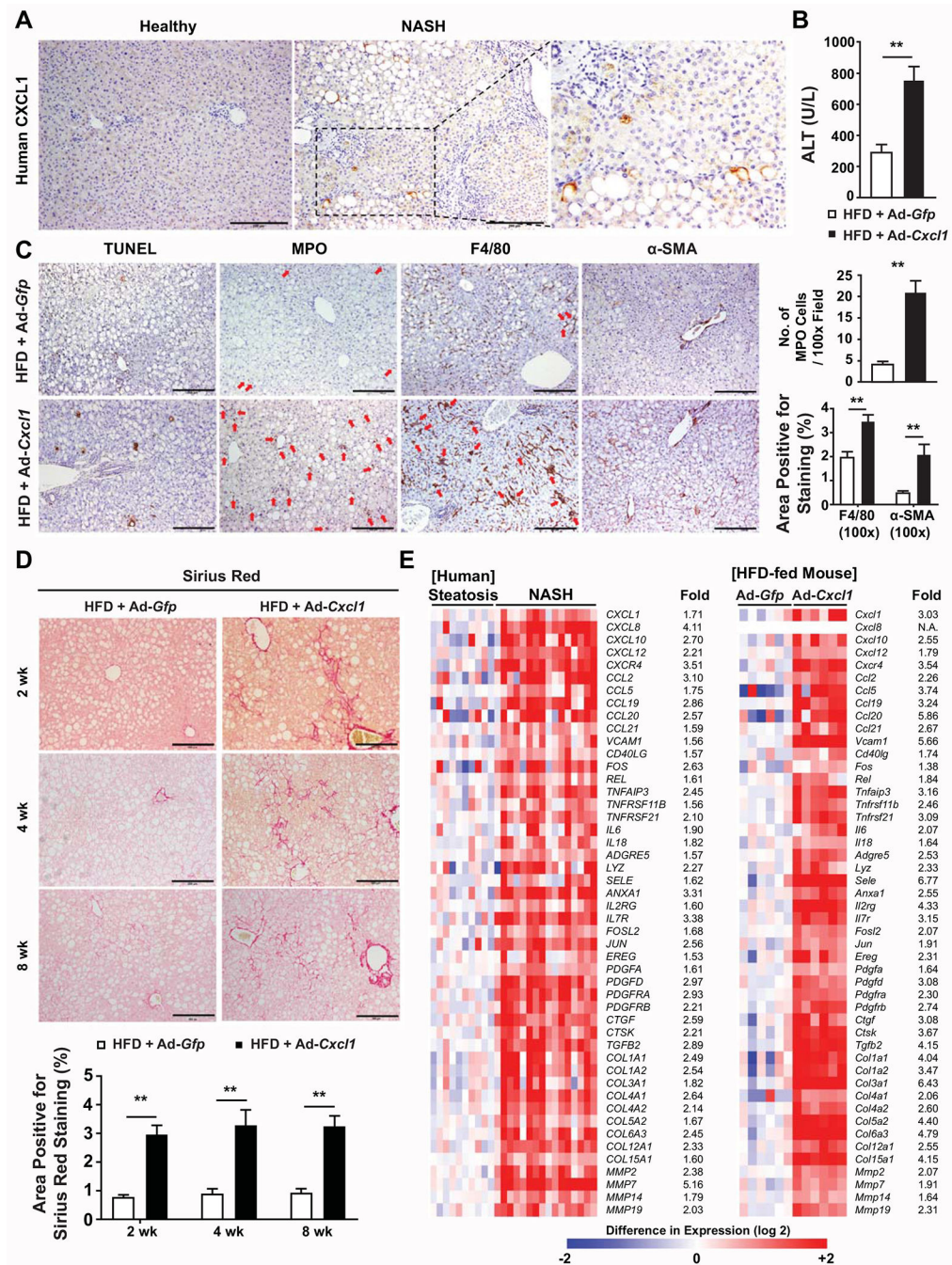


Fig. 1. Hepatic overexpression of CXCL1 promotes steatosis-to-NASH progression in HFD-fed mice.

(A) Immunohistochemical analysis of CXCL1 in the liver of healthy individuals and NASH patients. Representative images from 5 healthy individuals and 5 NASH patients are shown. Information for the characteristics of each patient is included in Supporting Table 1. (B-E) HFD-fed C57BL/6 mice were infected with Ad-Gfp or Ad-Cxcl1 for 2 weeks (in panels B-C, E) or up to 8 weeks (in panel D). (B) Serum ALT levels (n=6/group). (C) Representative images of various stainings in mouse liver sections (left) and the number of MPO-positive cells per field (100 \times) and the area positive for F4/80 staining and α -SMA staining (100 \times) in

liver sections (right). Red arrows indicate MPO⁺ cells (in MPO staining image) or hepatic crown-like structures (in F4/80 staining image). (D) Representative Sirius Red staining images in liver sections of HFD-fed mice infected with Ad-*Gfp* or Ad-*Cxcl1* for up to 8 weeks (top) and the quantification of the images (bottom). Scale bars indicate 200 μm . (E) Heat map illustration of the expression profiles of the genes involved in inflammation and fibrosis in human (left, obtained from microarray in Lake et al., *Drug Metab Dispos.* 2011;39:1954-1960) and 2-week Ad-*Gfp*- or Ad-*Cxcl1*-infected HFD-fed mice (right, obtained from RT-qPCR). Values represent mean \pm SEM. Statistical evaluation was performed by Student's t-test (** $p < 0.01$). N.A., not available.

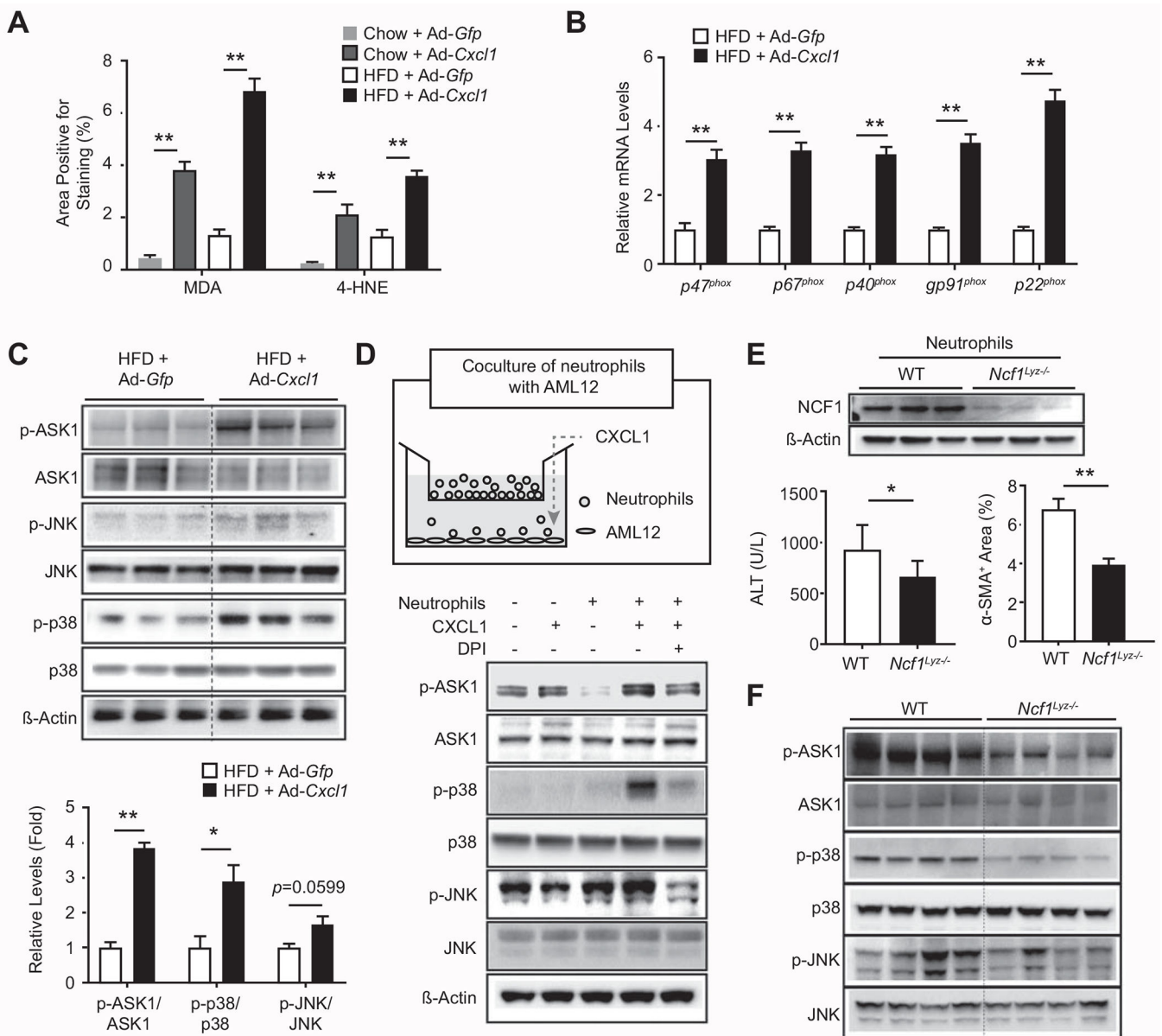


Fig. 2. Neutrophil infiltration mediates oxidative stress and liver injury in Ad-Cxcl1-infected, HFD-fed mice via an NCF1/p47^{phox}-dependent manner.

(A-C) HFD- or chow-fed C57BL/6 mice were infected with Ad-Gfp or Ad-Cxcl1 for 2 weeks. Quantification of the area positive for MDA staining or 4-HNE staining in liver sections is shown in panel A. The representative images are included in Supporting Fig. S5A. Expression of NADPH oxidase 2 complex in the liver was determined by RT-qPCR (n=6/group) in panel B. Hepatic expression of stress kinases was examined by immunoblot analysis (top) and the blots were quantified by densitometry (bottom) in panel C. (D) A schematic diagram depicting the coculture of neutrophils with AML12 (top) and the expression of stress kinases in AML12 cells (bottom). Neutrophils (1×10^6 cells) were placed onto the insert (3 μ m pore size), and a recombinant mouse CXCL1 protein (100 ng/mL) was added to the bottom chamber (6 hr). DPI (5 μ M) was added to the bottom chamber 30 min

prior to CXCL1 treatment. AML12 cells were then collected for immunoblot analysis. (E-F) HFD-fed *Ncf1^{Ly2z-/-}* and WT mice were infected with Ad-*Gfp* or Ad-*Cxcl1* for 2 weeks. Deletion of the *Ncf1* gene in bone marrow-derived neutrophils of *Ncf1^{Ly2z-/-}* mice was confirmed by immunoblot analysis (top, panel E). Serum ALT levels (bottom left, panel E) and quantification of α -SMA⁺ area (bottom right, panel E) from HFD-fed, Ad-*Cxcl1*-infected WT and *Ncf1^{Ly2z-/-}* mice. Representative α -SMA staining images are included in Supporting Fig. S5E. Hepatic expression of stress kinases was determined by immunoblot analysis in panel F. Values represent mean \pm SEM. Statistical evaluation was performed by Student's t-test or one-way ANOVA with Tukey's post hoc test for multiple comparisons (* $p < 0.05$; ** $p < 0.01$).

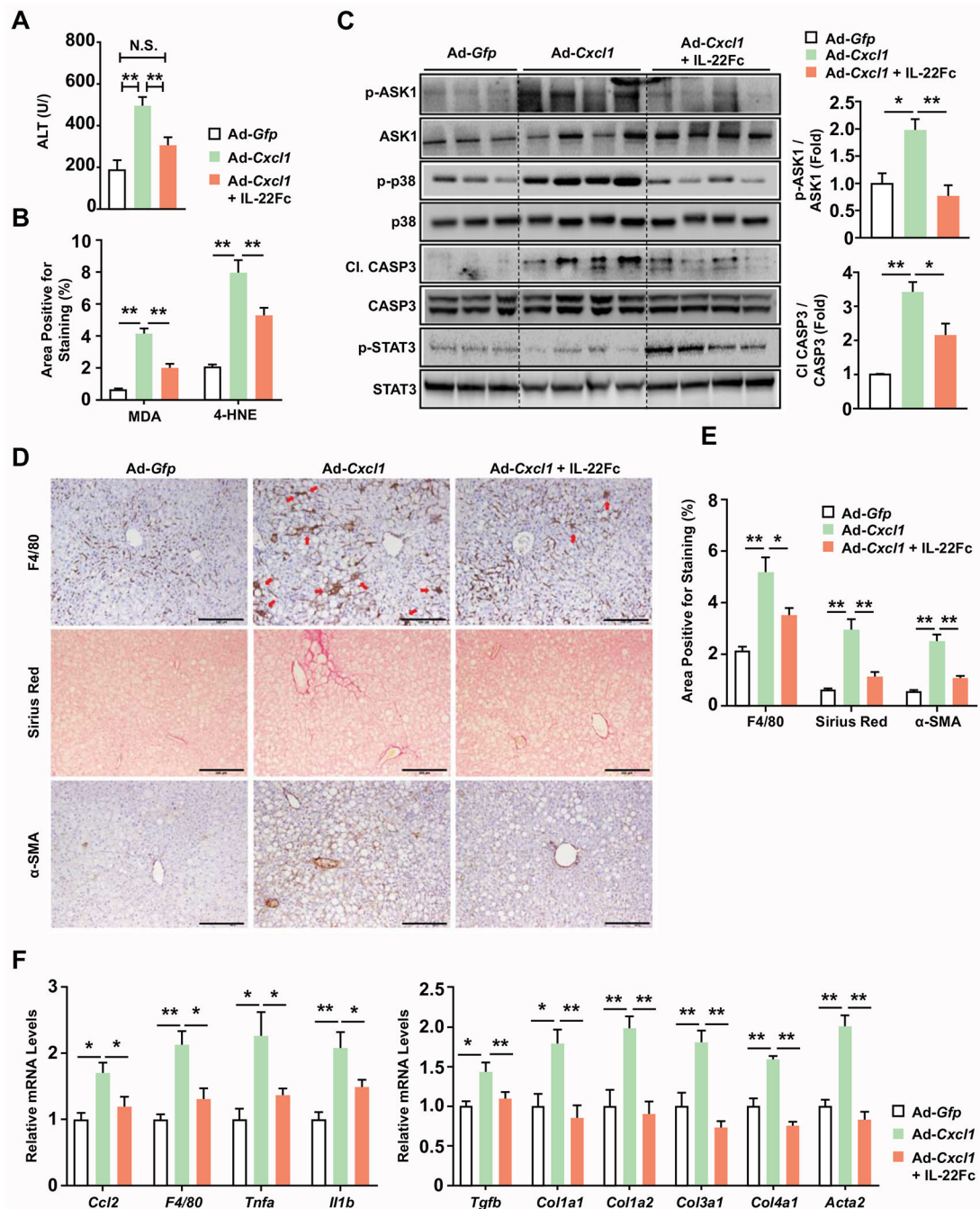


Fig. 3. IL-22Fc therapy ameliorates CXCL1-induced NASH in HFD-fed mice.

HFD-fed C57BL/6J mice were subjected to a 2-week infection with *Ad-Gfp* or *Ad-Cxcl1* and/or an IL-22Fc treatment. Detailed experimental design is illustrated in Supporting Fig. S7A. (A) Serum ALT levels (n=4-6/group). (B) Quantification of the area positive for MDA and 4-HNE staining. The representative images are included in Supporting Fig. S8A. (C) Hepatic expression of stress kinase, CASP3, and STAT3 was determined by immunoblot analysis (left) and the blots were quantified by densitometry (right). (D) Histological analysis of collagen (Sirius Red) and the expression of F4/80 and α-SMA. Red arrows

indicate hepatic crown-like structures. Scale bars indicate 200 μm . (E) Quantification of the histological analysis of F4/80, Sirius Red, and α -SMA included in panel (D). (F) RT-qPCR analysis of hepatic expression of inflammatory (left) and fibrogenic (right) genes (n=4-6/group). Values represent mean \pm SEM. Statistical evaluation was performed by one-way ANOVA with Tukey's post hoc test for multiple comparisons (* p <0.05; ** p <0.01). N.S., not significant; C1. CASP3, cleaved form of CASP3.

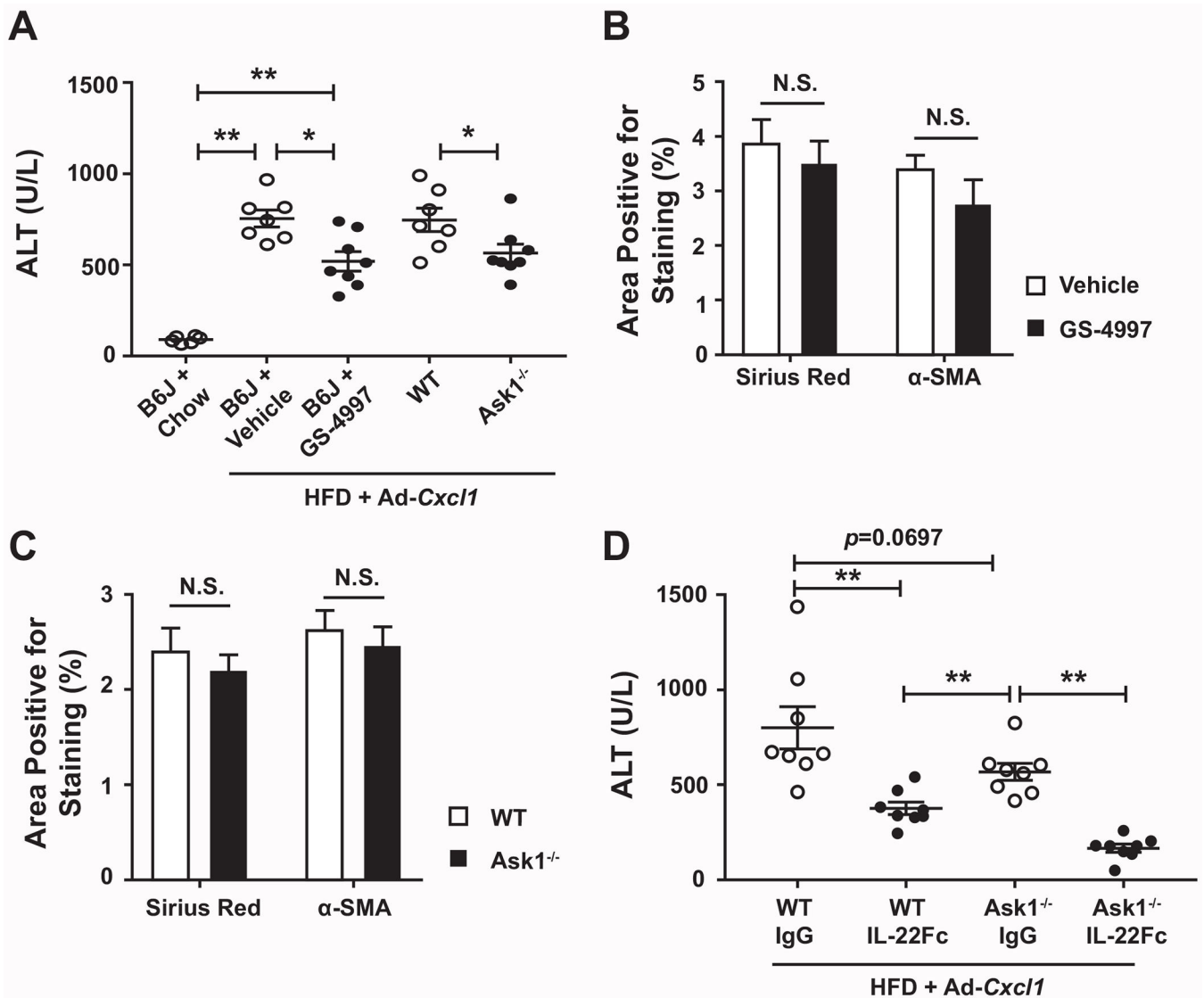


Fig. 4. ASK1 inhibition fails to ameliorate CXCL1-induced NASH and IL-22Fc improves NASH in an ASK1-independent manner. (A-C) HFD-fed C57BL/6J mice (B6J), *Ask1*^{-/-} mice and their WT littermates were infected with Ad-*Cxcl1* for two weeks. B6J group was also given vehicle or GS-4997 treatment (n=7–8/group). (A) Serum ALT levels. (B) Quantification of the histological analysis of Sirius Red and α-SMA in liver sections. The representative images are included in Supporting Fig. S11. (C) Quantification of the histological analysis of liver fibrosis in *Ask1*^{-/-} mice and WT littermates. The representative images are included in Supporting Fig. S12. (D) *Ask1*^{-/-} mice and WT littermates were given HFD + Ad-*Cxcl1*, followed by a treatment with IgG2 or IL-22Fc (n=8/group). Serum ALT levels were measured. Values represent mean ± SEM. Statistical evaluation was performed by Student's t-test or one-way ANOVA with Tukey's post hoc test for multiple comparisons (**p*<0.05; ***p*<0.01).

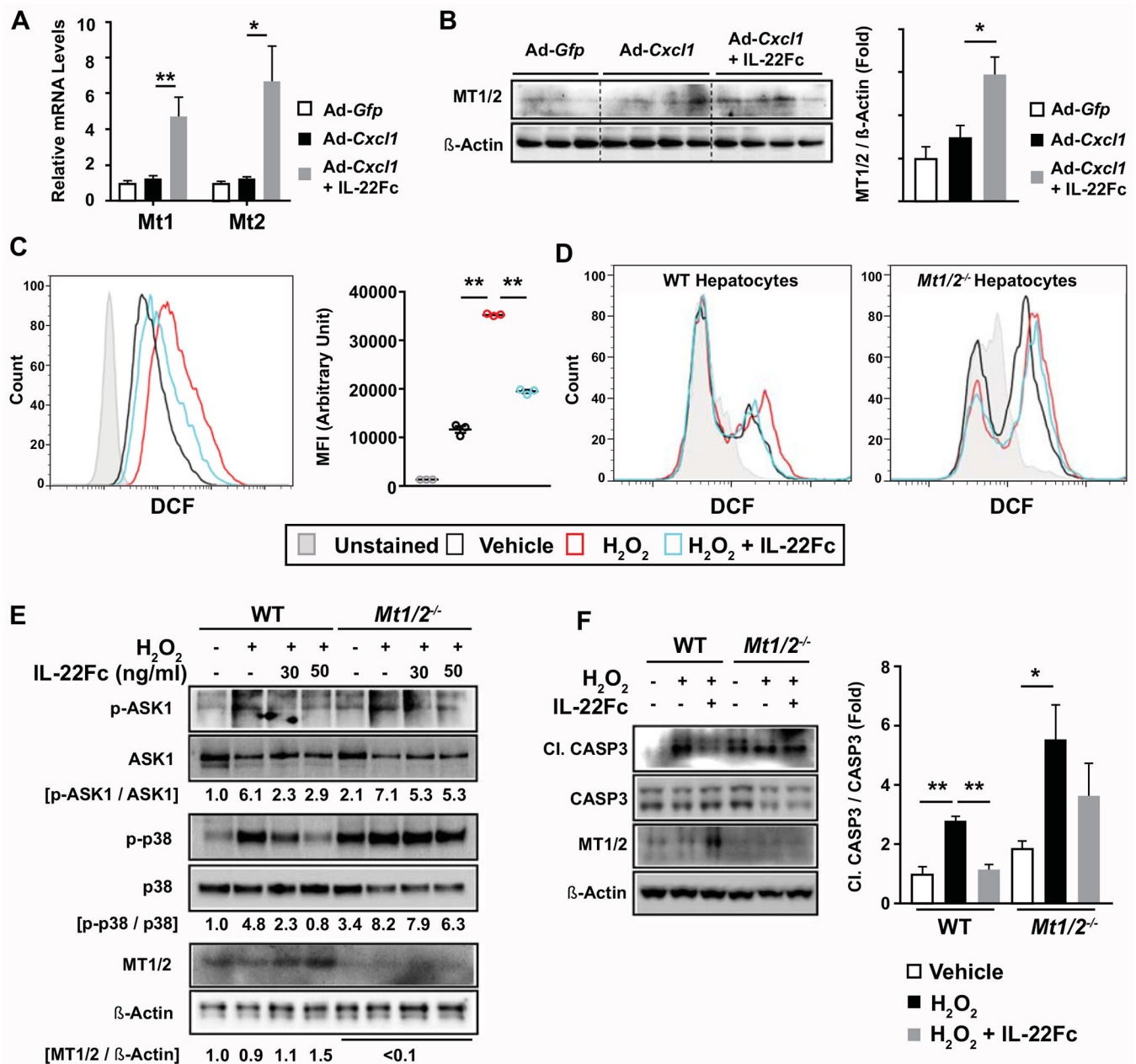


Fig. 5. MT contributes to the ability of IL-22Fc to attenuate ROS levels, stress kinase activation, and apoptotic signaling in hepatocytes.

(A, B) HFD-fed C57BL/6 mice were given Ad-Gfp, Ad-Cxcl1, or Ad-Cxcl1 + IL-22Fc (n=4-6/group). RT-qPCR (panel A) and immunoblot (panel B) analysis of hepatic mRNA and protein levels of *Mt1* and *Mt2*, respectively. (C) AML12 cells were pretreated with IL-22Fc for 20 hr, exposed to H₂O₂ for 2 hr, and subjected to flow cytometric analysis of DCF. Results obtained from cells untreated with DCFDA dye represent the unstained condition. MFI represents the mean fluorescence intensity of triplicates. (D-F) Primary WT and *Mt1/2*^{-/-} hepatocytes were pretreated with IL-22Fc for 20 hr, followed by a treatment with H₂O₂ for 30 min (panel D), 10 min (panel E), and 5 hr (panel F). ROS was measured by flow cytometric analysis of DCF (panel D). Immunoblot analyses were performed

(panels E, F). Quantification of the CASP3 cleavage normalized to intact CASP3 from three independent experiments are shown in panel F (right). Values represent mean \pm SEM. Statistical evaluation was performed by one-way ANOVA with Tukey's post hoc test for multiple comparisons (* p <0.05; ** p <0.01).

Author Manuscript

Author Manuscript

Author Manuscript

Author Manuscript

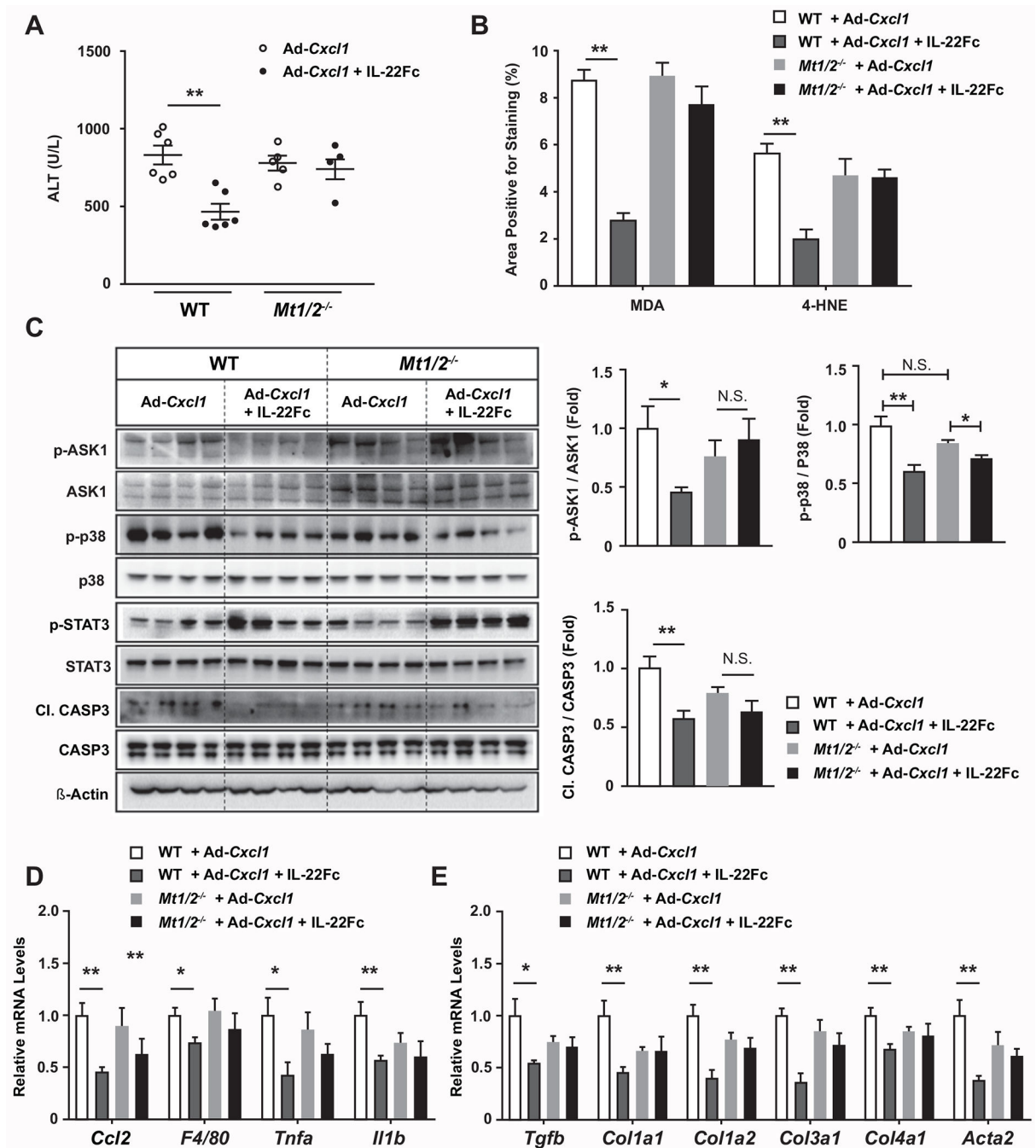


Fig. 6. IL-22Fc ameliorates CXCL1-induced NASH phenotypes in an MT-dependent manner. HFD-fed WT and *Mt1/2^{-/-}* mice were treated with *Ad-Cxcl1* and subsequently with IgG2 or IL-22Fc in accordance with the experimental design illustrated in Supporting Fig. S7A (n=5–6/group). (A) Serum ALT levels. (B) Paraffin-embedded liver sections were subjected to MDA and 4-HNE staining and the area positive for MDA or 4-HNE staining was quantified. The representative images of each staining are included in Supporting Fig. S15C. (C) Hepatic expression of ASK1, p38, STAT3, and CASP3 was determined by immunoblot analysis (left) and the blots were quantified by densitometry (right). (D, E) Hepatic

expression of inflammatory (panel D) and fibrogenic (panel E) genes was examined by RT-qPCR analysis. Values represent mean \pm SEM. Statistical evaluation was performed by one-way ANOVA with Tukey's post hoc test for multiple comparisons (* p <0.05; ** p <0.01).

Author Manuscript

Author Manuscript

Author Manuscript

Author Manuscript

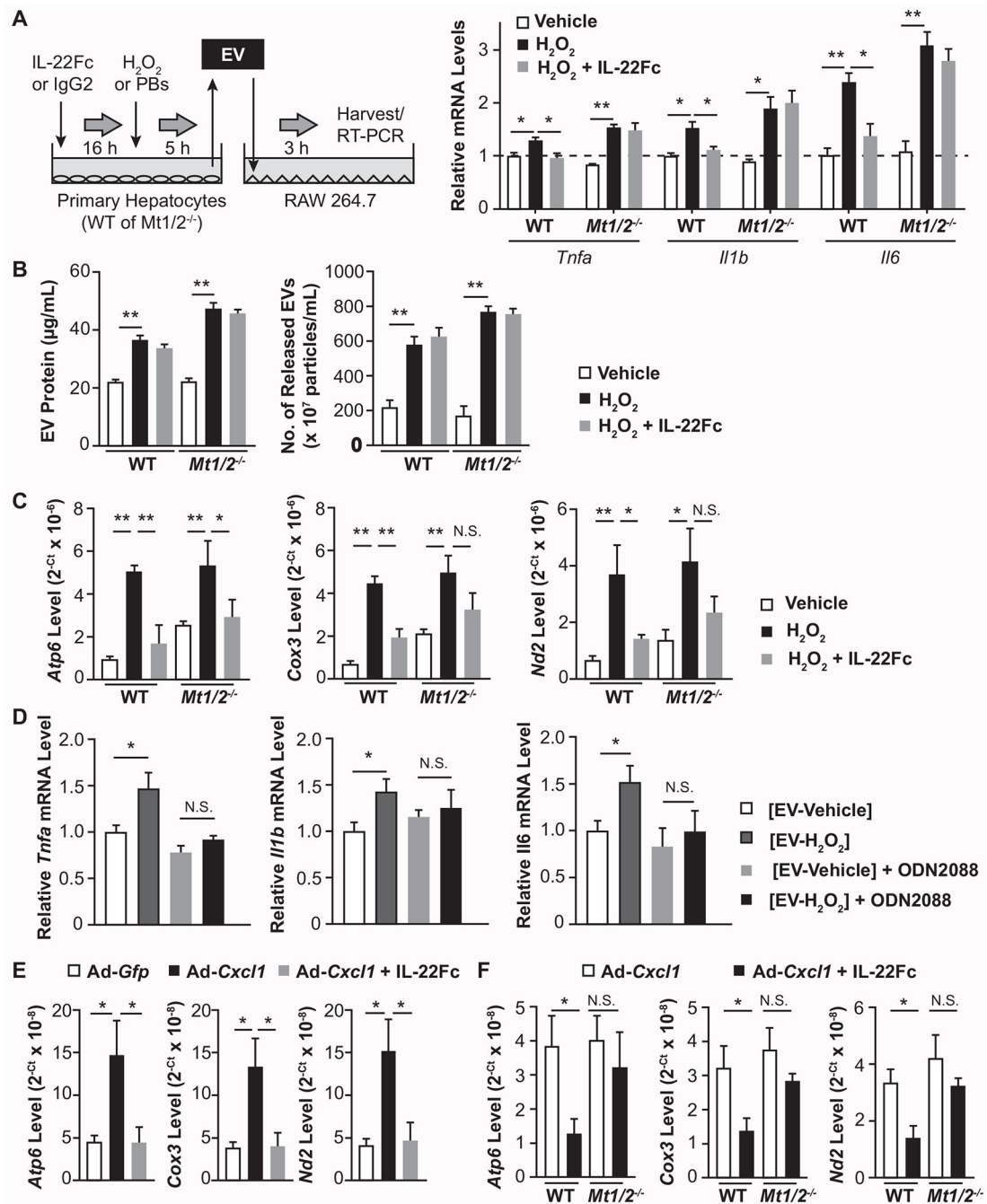


Fig. 7. IL-22Fc reduces the inclusion of mtDNA in EVs and inhibits their inflammatory properties in an MT-dependent manner.

(A) A schematic illustration of the treatment of RAW264.7 cells with hepatocyte-derived EVs (left). Mouse primary hepatocytes were treated with IL-22Fc or IgG2 followed by a treatment with H₂O₂ or PBS. EVs from culture medium were isolated and incubated with RAW264.7 cells (5 μg/mL, 3 hr), and RT-qPCR analysis of inflammatory genes was performed (n=3; right). (B) The amount of EVs isolated from primary hepatocytes was measured by BCA assay that quantifies EV protein (left) and EXOCET kit that measures the number of EVs based on the activity of EV-enriched acetylcholinesterase (right). (C) DNA

isolated from hepatocyte-derived EVs was subjected to qPCR using the primers for *Atp6*, *Cox3*, and *Nd2*. (D) RAW264.7 cells were pretreated with control or ODN2088 (2 μ M, 1 hr), treated with EVs (5 μ g/mL, 3 hr) from hepatocytes exposed to vehicle or H₂O₂ for 5 hr, and subjected to RT-qPCR analysis of inflammatory genes (n=4). (E, F) DNA extracted from the serum EVs of mice given Ad-*Gfp*, Ad-*Cxcl1*, or Ad-*Cxcl1* + IL-22Fc was subjected to qPCR to measure the levels of *Atp6*, *Cox3*, and *Nd2* (n=5–6/group). Values represent mean \pm SEM. Statistical evaluation was performed by one-way ANOVA with Tukey's post hoc test for multiple comparisons (* p <0.05; ** p <0.01).

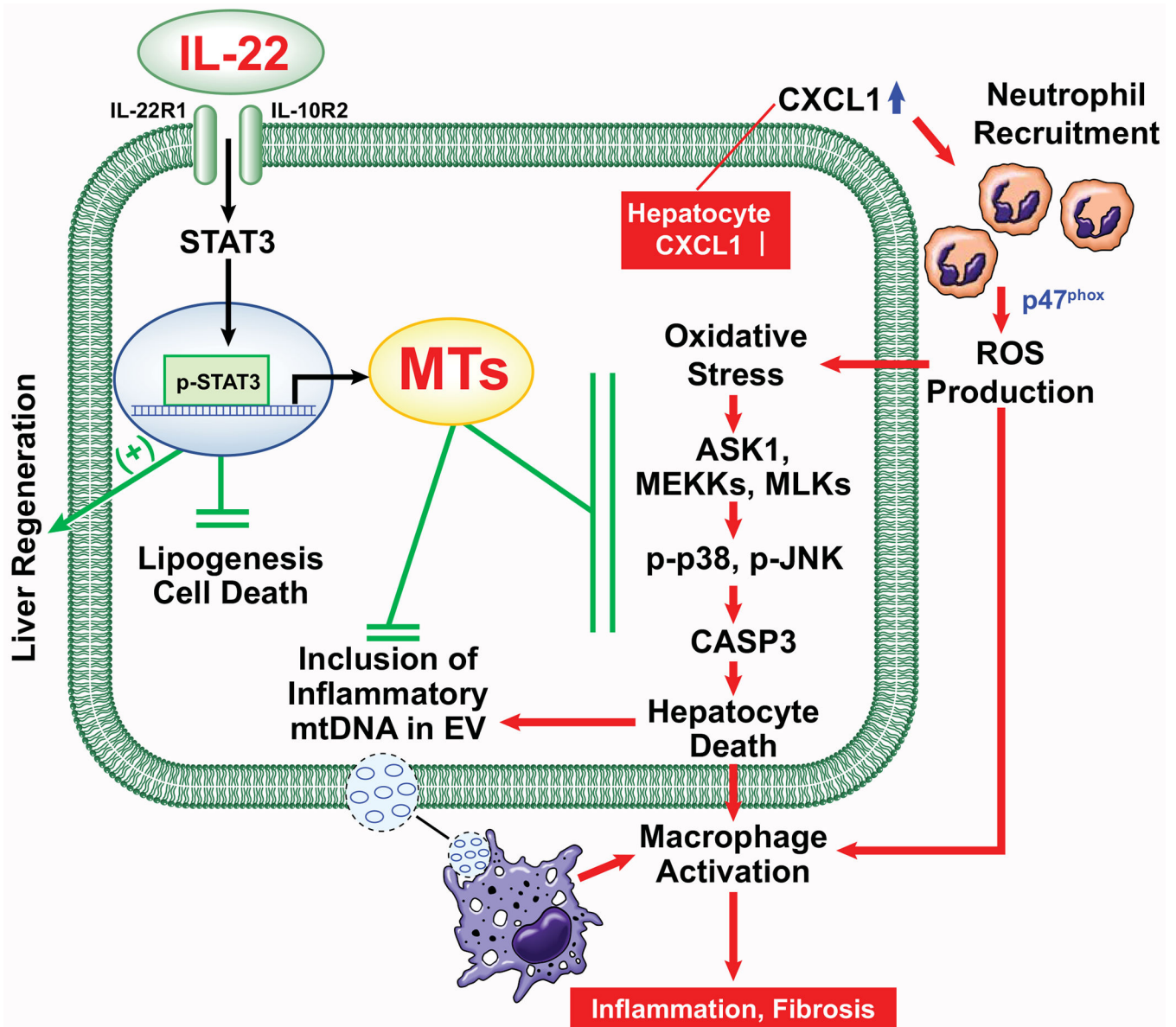


Fig. 8. A model depicting the therapeutic intervention of neutrophil-driven NASH by IL-22Fc that acts on multiple targets.

Adenoviral overexpression of CXCL1 in hepatocytes stimulates hepatic neutrophil infiltration and ROS production in a p47^{phox}-dependent manner, which activates ROS-sensitive kinases (ASK1, MEKKs, and MLKs) and their downstream stress kinases (p38 and JNK) and subsequently enhances apoptotic signaling involving CASP3 cleavage. ROS-damaged hepatocytes enhance inflammation by releasing mtDNA-including EVs that activate macrophages. IL-22Fc alleviates CXCL1-induced NASH by attenuating hepatocyte death, inflammation, and fibrosis through MT induction in addition to its MT-independent effects (e.g., liver regeneration and inhibition of lipogenesis and cell death).